

# Beam Wander of the Multi-Gaussian Schell-Model Beam in Anisotropic Turbulence

Jie Shu<sup>1</sup>, Huafeng Xu<sup>2</sup>, Zheng-Lan Zhou<sup>1</sup>, and Jun Qu<sup>1, \*</sup>

**Abstract**—Based on the extended Huygens-Fresnel principle, the expressions of degree of coherence, ellipticity, and beam wander of multi-Gaussian Schell-model beam through the anisotropic turbulence are derived. Their statistical properties in anisotropic turbulence are illustrated numerically. The results show that the beam width and beam wander of multi-Gaussian Schell-model beam decrease with the increase of the mode order or the decrease of the turbulence structure parameter and initial coherence and that the degree of coherence of multi-Gaussian Schell-model beam decreases with the increase of the turbulence structure parameter or the decrease of the mode order. Furthermore, the beam wander of multi-Gaussian Schell-model beam is smaller than that of Gaussian Schell-model beam under the same conditions.

## 1. INTRODUCTION

In the past decades, the propagation properties of beams in turbulent atmosphere have been studied in detail both theoretically and experimentally. More and more attention has been paid to the partially coherent beams propagating in free space and isotropic random media [1, 2]. Since the sufficient conditions for devising genuine correlation functions of scalar and vector partially coherent beams were discussed by Gori and collaborators [3], the propagation characteristics of partially coherent beams, such as multi-Gaussian Schell-model (MGSM) beam [4], Laguerre-Gaussian Schell-model beam [5], and Bessel-Gaussian Schell-model beam [6], have been proposed and studied.

It is well known that random variations of the refractive index of atmosphere can cause beam spreading, beam wander, and scintillations of beams, which affect the quality of beam seriously [7], and it should be considered in the application of laser communication. To our knowledge, the beam wander of coherent Gaussian beam [8] and partially coherent Gaussian Schell-model (GSM) beam [9] have been researched extensively, based on the turbulence theory of the refractive power spectrum of Kolmogorov [10, 11]. Lots of researches show that atmospheric turbulence is anisotropic rather than isotropic in the actual situation [12–15]. In other words, anisotropy models are more accurately compared to isotropic models.

Expressly, Wang et al. proposed a generalized multi-Gaussian Schell-model beam [16]. The first kind of it generates a dark hollow beam profile, and the other generates a flat-topped beam profile in the far field. Korotkova and her collaborators studied the propagation properties of MGSM beams in free space and isotropic random media [4], and Yuan et al. discussed the scintillation factor of MGSM beams propagation in atmospheric turbulence, and the results show that the scintillation indices of higher order MGSM beams are smaller than that of GSM beams [17].

In view of this, based on the extended Huygens-Fresnel principle, the analytical expressions of the spectral density (SD), degree of coherence (DOC), and beam wander of MGSM beam in anisotropic

---

*Received 6 December 2018, Accepted 8 February 2019, Scheduled 11 February 2019*

\* Corresponding author: Jun Qu (qujun70@ahnu.edu.cn).

<sup>1</sup> College of Physics and Electronic Information, Anhui Normal University, Wuhu, Anhui 241000, China. <sup>2</sup> School of Mechanics and Photoelectric Physics, Anhui University of Science and Technology, Huainan, Anhui 232001, China.

turbulence are given in this paper. The theoretical results may be useful for the potential applications of MGSM beam in free-space optical communications.

## 2. THEORETICAL MODEL

### 2.1. DOC, Beam Spreading and Ellipticity

The expression of the generalized Huygens-Fresnel diffraction integral formula is as follows

$$E(\boldsymbol{\rho}, z) = \frac{\exp(ikz)}{i\lambda z} \int_{-\infty}^{\infty} E(\mathbf{r}, 0) \exp\left[-\frac{ik}{2z}(\boldsymbol{\rho} - \mathbf{r})^2\right] \exp[\Psi(\mathbf{r}, \boldsymbol{\rho}, z)] d^2\mathbf{r}. \quad (1)$$

Here  $k = 2\pi/\lambda$  is the wavenumber at the wavelength of  $\lambda$ , and  $\Psi(\mathbf{r}, \boldsymbol{\rho}, z)$  is the complex phase perturbation of a spherical wave propagating through the anisotropic turbulence from  $(\mathbf{r}, 0)$  to  $(\boldsymbol{\rho}, z)$ .

The cross-spectral density (CSD) function of the MGSM beam in the source field is [18]

$$\begin{aligned} W^{(0)}(\mathbf{r}_1, \mathbf{r}_2) &= \langle E(\mathbf{r}_1, 0) E^*(\mathbf{r}_2, 0) \rangle \\ &= \frac{1}{C_0} \exp\left(-\frac{\mathbf{r}_1^2 + \mathbf{r}_2^2}{4\sigma_0^2}\right) \sum_{m=1}^M \binom{M}{m} \frac{(-1)^{m-1}}{m} \exp\left[-\frac{(\mathbf{r}_1 - \mathbf{r}_2)^2}{2m\delta_0^2}\right], \end{aligned} \quad (2)$$

where  $\mathbf{r}_1$  and  $\mathbf{r}_2$  are two arbitrary points in the source plane,  $C_0 = \sum_{m=1}^M \binom{M}{m} \frac{(-1)^{m-1}}{m}$  is the normalization factor with  $M$  being the beam index;  $\sigma_0$  denotes the transverse beam width of the source plane;  $\delta_0$  denotes the initial coherence width; and  $M$  is the beam index.

According to Eqs. (1) and (2), the CSD function of an MGSM beam after propagating through anisotropic turbulence at distance  $z$  is [19]

$$\begin{aligned} W(\boldsymbol{\rho}_1, \boldsymbol{\rho}_2, z) &= \frac{1}{\lambda^2 z^2} \int_{-\infty}^{\infty} \int_{-\infty}^{\infty} W^{(0)}(\mathbf{r}_1, \mathbf{r}_2) \exp\left[-\frac{ik}{2z}(\boldsymbol{\rho}_1 - \mathbf{r}_1)^2 + \frac{ik}{2z}(\boldsymbol{\rho}_2 - \mathbf{r}_2)^2\right] \\ &\quad \times \langle \exp[\Psi^*(\mathbf{r}_1, \boldsymbol{\rho}_1, z) + \Psi(\mathbf{r}_2, \boldsymbol{\rho}_2, z)] \rangle d^2\mathbf{r}_1 d^2\mathbf{r}_2, \end{aligned} \quad (3)$$

here  $\boldsymbol{\rho}_1 \equiv (\xi_1, \eta_1)$  and  $\boldsymbol{\rho}_2 \equiv (\xi_2, \eta_2)$  denote two arbitrary points in the plane  $z > 0$ , and  $\Psi^*(\mathbf{r}, \boldsymbol{\rho}, z)$  denotes complex conjugate [19]

$$\langle \exp[\Psi^*(\mathbf{r}_1, \boldsymbol{\rho}_1, z) + \Psi(\mathbf{r}_2, \boldsymbol{\rho}_2, z)] \rangle = \exp\left[-\frac{\pi^2 k^2 z T (\xi_d^2 + \xi_d x_d + x_d^2)}{3\mu_x^2}\right] \exp\left[-\frac{\pi^2 k^2 z T (\eta_d^2 + \eta_d y_d + y_d^2)}{3\mu_y^2}\right], \quad (4)$$

The power spectrum is chosen as [19]

$$\Phi'_n(\kappa') = \mu_x \mu_y \mu_z A(\alpha) \tilde{C}_n^2 \left(|\kappa'|^2 + \kappa_0^2\right)^{-\frac{\alpha}{2}} \exp\left(-\frac{|\kappa'|^2}{\kappa_m^2}\right). \quad (5)$$

And

$$T = \int_0^{\infty} d\kappa' \kappa'^3 \Phi'_n(\kappa') / \mu_x \mu_y = \frac{\mu_z A(\alpha)}{2(\alpha - 2)} \tilde{C}_n^2 [\beta \kappa_m^{2-\alpha} \exp(\kappa_0^2/\kappa_m^2) \Gamma_1(2 - \alpha/2, \kappa_0^2/\kappa_m^2) - 2\kappa_0^{4-\alpha}]. \quad (6)$$

$\kappa' \equiv (\kappa'_x, \kappa'_y)$ ,  $\kappa_0 = 2\pi/L_0$ ,  $\kappa_m = c(\alpha)/l_0$ ,  $\beta = 2\kappa_0^2 - 2\kappa_m^2 + \alpha\kappa_m^2$ .  $\boldsymbol{\rho}_d = \boldsymbol{\rho}_1 - \boldsymbol{\rho}_2$ ;  $\tilde{C}_n^2$  is a generalized structure parameter of refractive index with unit  $m^{3-\alpha}$ ;  $A(\alpha) = \Gamma(\alpha - 1) \cos(\alpha\pi/2)/4\pi^2$ ;  $\alpha$  is the non-Kolmogorov slope;  $\Gamma_1(\cdot, \cdot)$  denotes the incomplete Gamma function;  $\Phi'_n(\kappa)$  is the spectral power spectrum of the refractive-index fluctuation in turbulence;  $\mu_x$  and  $\mu_y$  are the anisotropic factors in two transverse directions; and  $\mu_z$  is the anisotropic factor in direction of propagation.

Substituting Eqs. (2), (4), (5), and (6) into Eq. (3) and complex operation, we obtain the following expression for the CSD of MGSM beam in the receiver plane in turbulent atmospheric [19]

$$W(\boldsymbol{\rho}_1, \boldsymbol{\rho}_2, z) = W_x(\xi_1, \xi_2) W_y(\eta_1, \eta_2), \quad (7)$$

with

$$\begin{aligned}
 W_x(\xi_1, \xi_2) = & \frac{1}{C_0} \sum_{m=1}^M \frac{(-1)^{m-1}}{m} \binom{M}{m} \frac{1}{\sqrt{\Delta_x(z)}} \exp \left[ -\frac{1}{4\sigma_0^2 \Delta_x(z)} (\xi_1^2 + \xi_2^2) \right] \\
 & \times \exp \left\{ \left[ \frac{ik}{2z} \left( \frac{1}{\Delta_x(z)} - 1 \right) + \frac{i\pi^2 k z^2 T}{3\mu_x^2 \Delta_x(z)} \left( \frac{\pi^2 k^2 z T}{3\mu_x^2} + \frac{1}{2m\delta_0^2} - \frac{1}{4\sigma_0^2} \right) \right] (\xi_1^2 - \xi_2^2) \right\} \\
 & \times \exp \left\{ - \left[ \frac{1}{2m\delta_0^2 \Delta_x(z)} + \frac{\pi^2 k^2 z T}{3\mu_x^2} \left( 1 + \frac{2}{\Delta_x(z)} \right) - \frac{\pi^4 k^2 z^4 T^2}{18\mu_x^4 \Delta_x(z) \sigma_0^2} \right] (\xi_1 - \xi_2)^2 \right\}.
 \end{aligned} \tag{8}$$

The parameter  $\Delta_x(z)$  in Eq. (8) is

$$\Delta_x(z) = 1 + \left( \frac{1}{4\sigma_0^4} + \frac{1}{m\delta_0^2 \sigma_0^2} + \frac{2\pi^2 k^2 z T}{3\mu_x^2 \sigma_0^2} \right) \frac{z^2}{k^2}. \tag{9}$$

In the above derivation, the following integral formula is used [20]

$$\int_{-\infty}^{\infty} \exp(-p^2 x^2 \pm qx) dx = \frac{\sqrt{\pi}}{p} \exp\left(\frac{q^2}{4p^2}\right). \tag{10}$$

The factor  $W_y(\eta_1, \eta_2)$  has the same form as  $W_x(\xi_1, \xi_2)$

$$\begin{aligned}
 W_y(\eta_1, \eta_2) = & \frac{1}{C_0} \sum_{m=1}^M \frac{(-1)^{m-1}}{m} \binom{M}{m} \frac{1}{\sqrt{\Delta_y(z)}} \exp \left[ -\frac{1}{4\sigma_0^2 \Delta_y(z)} (\eta_1^2 + \eta_2^2) \right] \\
 & \times \exp \left\{ \left[ \frac{ik}{2z} \left( \frac{1}{\Delta_y(z)} - 1 \right) + \frac{i\pi^2 k z^2 T}{3\mu_y^2 \Delta_y(z)} \left( \frac{\pi^2 k^2 z T}{3\mu_y^2} + \frac{1}{2m\delta_0^2} - \frac{1}{4\sigma_0^2} \right) \right] (\eta_1^2 - \eta_2^2) \right\} \\
 & \times \exp \left\{ - \left[ \frac{1}{2m\delta_0^2 \Delta_y(z)} + \frac{\pi^2 k^2 z T}{3\mu_y^2} \left( 1 + \frac{2}{\Delta_y(z)} \right) - \frac{\pi^4 k^2 z^4 T^2}{18\mu_y^4 \Delta_y(z) \sigma_0^2} \right] (\eta_1 - \eta_2)^2 \right\}.
 \end{aligned} \tag{11}$$

The parameter  $\Delta_y(z)$  in Eq. (11) is

$$\Delta_y(z) = 1 + \left( \frac{1}{4\sigma_0^4} + \frac{1}{m\delta_0^2 \sigma_0^2} + \frac{2\pi^2 k^2 z T}{3\mu_y^2 \sigma_0^2} \right) \frac{z^2}{k^2}. \tag{12}$$

From [19]

$$S(\rho, z) = W(\rho, \rho, z), \tag{13}$$

$$\mu(\rho_1, \rho_2, z) = \frac{W(\rho_1, \rho_2, z)}{\sqrt{S(\rho_1, z) S(\rho_2, z)}}. \tag{14}$$

We obtain the following expression for the beam width and coherence width of MGSM beam along  $x$  ( $y$ ) direction

$$\begin{aligned}
 l\sigma_i(z) &= \sigma_0 \sqrt{\Delta_i(z)} \\
 &= \sqrt{\frac{z^2}{4k^2 \sigma_0^2} + \frac{z^2}{mk^2 \delta_0^2} + \frac{2\pi^2 z^3 T}{3\mu_i^2} + \sigma_0^2}, \quad (i = x, y),
 \end{aligned} \tag{15}$$

$$\delta_i(z) = \left[ \frac{1}{m\delta_0^2 \Delta_i(z)} + \frac{2\pi^2 k^2 z T}{3\mu_i^2} + \frac{2\pi^2 k^2 z T}{3\mu_i^2 \Delta_i(z)} \left( 2 - \frac{\pi^2 z^3 T}{6\mu_i^2 \sigma_0^2} \right) \right]^{-1/2}, \quad (i = x, y). \tag{16}$$

In order to quantitatively analyze the changes of the SD and DOC of the MGSM beam propagating in the anisotropic turbulence, ellipticity is defined as [19]

$$f(z) = \frac{P(z) - Q(z)}{P(z)}. \tag{17}$$

Form Eq. (17),  $P(z)$  ( $Q(z)$ ) denotes the r.m.s. beam width (or coherence width) along  $x$  ( $y$ ) direction, and  $f(z)$  satisfies  $0 \leq f(z) < 1$ . The ellipse is reduced to a circle when  $f(z) = 0$ . The larger the value of  $f(z)$  is, the larger the ellipticity is. Under the condition  $\mu_x > \mu_y$ , the ellipticities of the SD and DOC are expressed as  $(\sigma_y(z) - \sigma_x(z))/\sigma_y(z)$  and  $(\delta_x(z) - \delta_y(z))/\delta_x(z)$ .

## 2.2. Beam Wander

Beam wander is an important characteristic of laser beams, defined as [21]

$$\langle r_c^2 \rangle = 4\pi k^2 W_{FS}^2 \int_0^L \int_0^\infty \kappa \Phi_n(\kappa) \exp[-\kappa^2 W_{LT}^2] \left\{ 1 - \exp\left[-\frac{2L^2 \kappa^2 (1-z/L)^2}{k^2 W_{FS}^2}\right] \right\} d\kappa dz, \quad (18)$$

$W_{LT}$  and  $W_{FS}$  are the beam radii with or without random media disturbed on propagation distance  $z$ ;  $L$  is the total propagation distance;  $\kappa$  is the spatial frequency. From [21], Eq. (18) can be expressed as follows

$$1 - \exp\left[-\frac{2L^2 \kappa^2 (1-z/L)^2}{k^2 W_{FS}^2}\right] \cong \frac{2L^2 \kappa^2 (1-z/L)^2}{k^2 W_{FS}^2} \quad L\kappa^2/k \ll 1. \quad (19)$$

Substituting Eqs. (15), (19), and (5) into Eq. (18), we can derive the beam wander of MGSM beam in turbulent atmosphere

$$\begin{aligned} \langle r_c^2 \rangle = & 8\pi L^2 \mu_z A(\alpha) \tilde{C}_n^2 \int_0^L (1-z/L)^2 dz \frac{1}{2(\alpha-2)} \frac{1}{C_0} \sum_{m=1}^M \frac{(-1)^{m-1}}{m} \binom{M}{m} \\ & \times \left\{ \begin{aligned} & -2\kappa_0^{4-\alpha} + \left(\frac{1}{\kappa_m^2} + W_{LT}^2\right)^{\frac{\alpha}{2}-1} \exp\left[\kappa_0^2 \left(\frac{1}{\kappa_m^2} + W_{LT}^2\right)\right] \\ & \times \left(2\kappa_0^2 + \frac{\alpha-2}{\frac{1}{\kappa_m^2} + W_{LT}^2}\right) \Gamma\left[2 - \frac{\alpha}{2}, \kappa_0^2 \left(\frac{1}{\kappa_m^2} + W_{LT}^2\right)\right] \end{aligned} \right\}, \quad (20) \end{aligned}$$

where the beam width of MGSM beam in anisotropic turbulence is

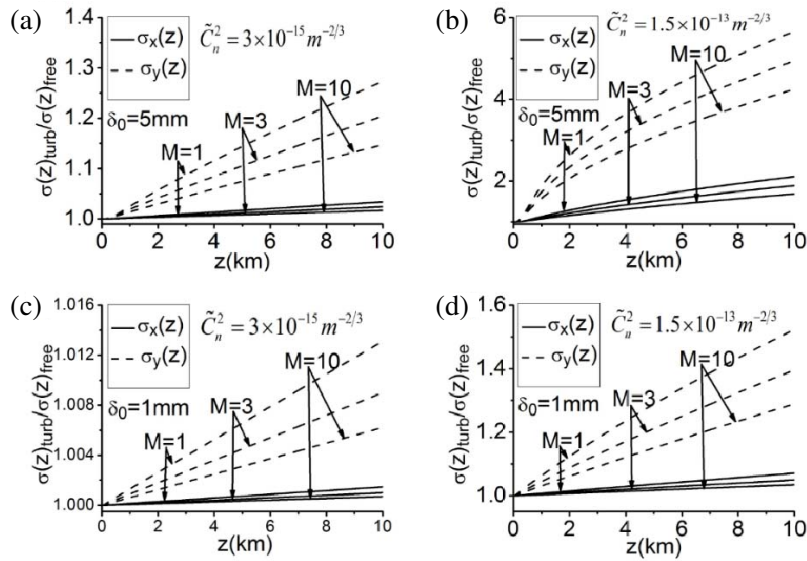
$$W_{LT}^2 = \sigma_0^2 + \frac{z^2}{4k^2 \sigma_0^2} + \frac{z^2}{mk^2 \delta_0^2} + \frac{2\pi^2 z^3 T}{3\mu_i^2}, \quad (i = x, y). \quad (21)$$

## 3. NUMERICAL EXAMPLES

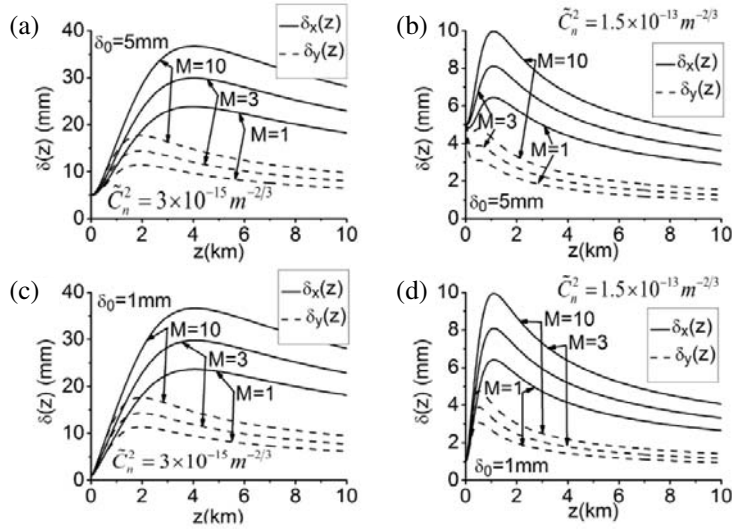
Based on Eqs. (13), (14), and (15), we illustrate the evolution of the beam width, SD, and DOC of MGSM beam propagation in anisotropic turbulence. The initial parameters in the numerical calculation are chosen to be  $\sigma_0 = 5$  mm,  $\lambda = 632.8$  nm,  $l_0 = 0.01$  m,  $L_0 = 1.0$  m,  $\mu_x = \mu_z = 3$ ,  $\mu_y = 1$ ,  $\alpha = 11/3$  and  $\tilde{C}_n^2 = 3 \times 10^{-14} \text{ m}^{3-\alpha}$  unless different values are specified.

Figure 1 shows the relationship between r.m.s. beam width and propagation distance for different orders of MGSM beams. It can be seen from Figs. 1(a) and 1(b) that the r.m.s. beam width of the higher order of the MGSM beam is smaller than that of the lower one under the same initial coherence. We also notice that the beam width in  $y$  direction is always larger than that in  $x$  direction. In addition, the r.m.s. beam width of the MGSM beam increases with further increase of turbulence structure parameter. As can be seen from Figs. 1(a) and 1(c), the r.m.s. beam width decreases with the further decrease of initial coherence. Fig. 1 also shows that under the same conditions, the beam width of the MGSM beam is smaller than that of the GSM beam, indicating that the MGSM beam can mitigate the effects of anisotropic turbulence.

Figure 2 shows the relationship between the r.m.s. DOC of MGSM beam and the propagation distance under different initial coherence and turbulence structure parameters. In Figs. 2(a) and 2(b), the r.m.s. DOC of GSM beam decreases with the further increase of turbulence structure parameter. From Figs. 2(a) and 2(c), one can see that the r.m.s. DOCs of MGSM beam in  $x$  and  $y$  directions are approximately equal when the propagation distance is less than about 1 km. Therefore, the MGSM beam is less affected by external interference, and the DOC is distributed in a circle over a short propagation distance, because of the diffraction by the initial coherence. The r.m.s. DOC of MGSM



**Figure 1.** R.m.s. beam widths in  $x$  and  $y$  directions of MGSM beam on propagation in turbulent anisotropic for different values of initial degree of coherence for  $\delta_0 = 5$  mm [(a), (b)],  $\delta_0 = 1$  mm [(c), (d)] and turbulence structure parameter for  $\tilde{C}_n^2 = 3 \times 10^{-15} m^{-2/3}$  [(a), (c)],  $\tilde{C}_n^2 = 1.5 \times 10^{-15} m^{-2/3}$  [(b), (d)].



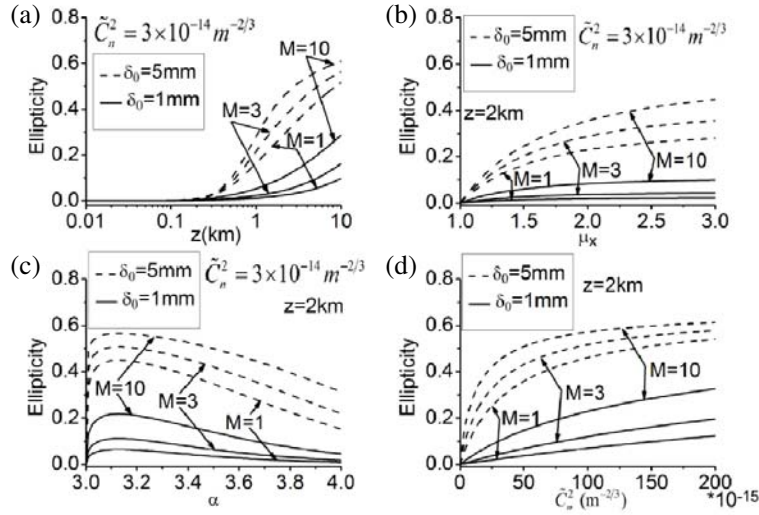
**Figure 2.** R.m.s. DOC in  $x$  and  $y$  directions of MGSM beam on propagation in turbulent anisotropic for different values of initial degree of coherence for  $\delta_0 = 5$  mm [(a), (b)],  $\delta_0 = 1$  mm [(c), (d)] and turbulence structure parameter for  $\tilde{C}_n^2 = 3 \times 10^{-15} m^{-2/3}$  [(a), (c)],  $\tilde{C}_n^2 = 1.5 \times 10^{-15} m^{-2/3}$  [(b), (d)].

beam increases with the further increase of propagation distance, and then the r.m.s. DOC of MGSM beam gradually decreases due to the de-coherence effect.

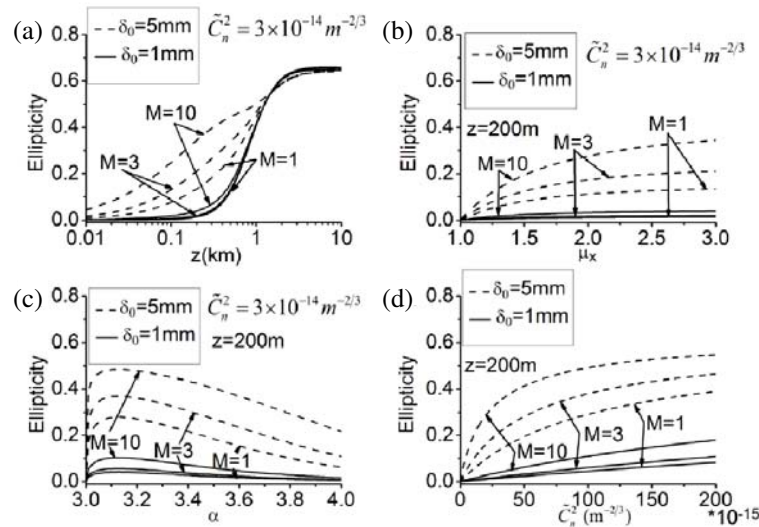
Figure 3(a) shows the dependence of the ellipticity of SD on the propagation distance. One can see that the SD of the MGSM beam on the cross section maintains a circular distribution as  $z \leq 1$  km, and then the SD of the MGSM beam transitions into an elliptical distribution gradually. Moreover, the SD of the higher order MGSM beam transitions into an elliptical distribution faster than the lower one. At fixed propagation distance of 2 km, the changes of the ellipticities of SD with the anisotropic factor  $\mu_x$  [see in Fig. 3(b)], the power law  $\alpha$  [see in Fig. 3(c)], and the turbulence structure parameter [see in

Fig. 3(d)] are shown. It is shown that the ellipticity of the SD increases with the increase of anisotropic factor, and in the range of the power law ( $3 < \alpha < 4$ ), the ellipticity of SD increases firstly and then decreases, and the ellipticity of SD increases with the further increase of turbulence structure parameter. Thus, the SD of MGSM beam has better ellipticity than that of the GSM beam under the same conditions.

Figure 4(a) illustrates the dependence of the ellipticities of DOC distribution on the propagation distance. The ellipticity of DOC distribution with small initial coherence approaches zero when the propagation distance is less than about 100 m and then increases with the further propagation distance, and ellipticity of DOC increases gradually. At fixed propagation of about 200 m, the changes of the ellipticity of DOC with the anisotropic factor  $\mu_x$  [see in Fig. 4(b)], the power law  $\alpha$  [see in Fig. 4(c)], and the turbulence structure parameter [see in Fig. 4(d)] are shown. It is found that the ellipticity of DOC



**Figure 3.** Changes of the ellipticity of SD with (a) propagation distance, (b) anisotropic factor  $\mu_x$ , (c) power law  $\alpha$  and (d) turbulence structure parameter.



**Figure 4.** Changes of the ellipticity of DOC distribution with (a) propagation distance, (b) anisotropic factor  $\mu_x$ , (c) power law  $\alpha$  and (d) turbulence structure parameter.

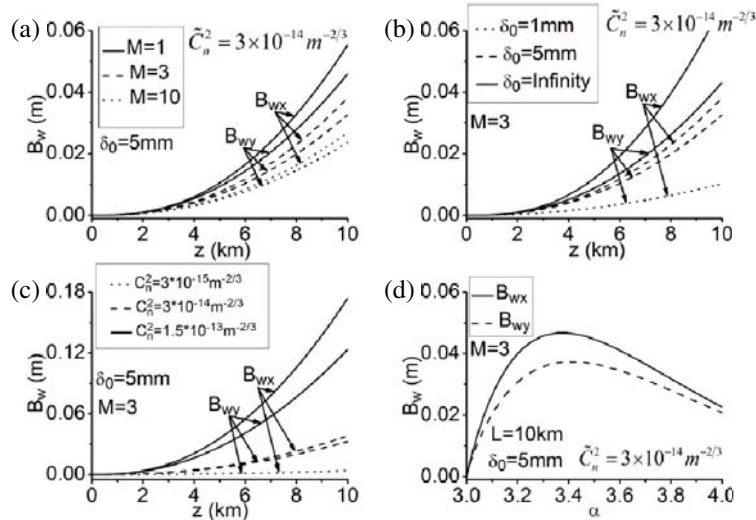


**Figure 5.** Changes of the beam wander of MGSM beam with (a) mode orders, (b) initial degree of coherence, (c) turbulence structure parameter and (d) power law  $\alpha$ .

increases with the further increase of anisotropic factor, and in the range of the power law ( $3 < \alpha < 4$ ), the ellipticity of DOC increases firstly and then decreases, and the ellipticity of DOC increases with the further increase of turbulence structure parameter.

Figure 5 illustrates the dependence of the beam wander of MGSM beam on the mode orders, initial degree of coherence, turbulence structure parameter, and power law. With the same initial coherence in Fig. 5(a), the beam wander of the highorder MGSM beam is smaller than that of the lower one with increasing propagation distance, and among the parameters are  $\tilde{C}_n^2 = 3 \times 10^{-14} \text{ m}^{-2/3}$ ,  $\delta_0 = 5 \text{ mm}$ . As seen from Fig. 5(b), under the same conditions of  $M = 3$ ,  $\tilde{C}_n^2 = 3 \times 10^{-14} \text{ m}^{-2/3}$ , when initial coherence decreases, the beam wander of MGSM beam decreases. The beam wander of MGSM beam decreases with the decrease of turbulence structure parameter when the initial coherence and order are constant. Under the same order and initial coherence, the beam wander of MGSM beam increases in the beginning and then decreases in the range of the power law ( $3 < \alpha < 4$ ). Thus, the beam wander of MGSM beam is smaller than that of the GSM beam under the same conditions in Fig. 5, and the MGSM beam is less affected by the anisotropic turbulence than the GSM beam as expected.

#### 4. CONCLUSION

In conclusion, based on the extended Huygens-Fresnel principle, the DOC, ellipticity, and beam wander of MGSM beam through turbulent anisotropy are derived. After the corresponding numerical calculation, its propagation distance is longer due to less coherence and beam wander than that of GSM beam. The beam width and beam wander of MGSM beam decrease with the increase of the mode order or the decrease of the turbulence structure parameter and initial coherence, and the DOC of MGSM beam decreases with the increase of the turbulence structure parameter or the decrease of mode order. The beam wander of MGSM beam will be smaller than that of GSM beam under the same conditions. Thus, the MGSM beam can mitigate the influence of the anisotropic turbulence. The conclusions obtained have certain reference significance for optical communication.

#### ACKNOWLEDGMENT

This work was supported by the National Natural Science Foundation of China (No. 11747065, No. 11374015).

## REFERENCES

1. Shirai, T., A. Dogariu, and E. Wolf, "Directionality of Gaussian Schell-model beams propagating in atmospheric turbulence," *Opt. Lett.*, Vol. 28, No. 8, 610, 2003.
2. Wu, G., H. Guo, S. Yu, and B. Luo, "Spreading and direction of Gaussian-Schell model beam through a non-Kolmogorov turbulence," *Opt. Lett.*, Vol. 35, No. 5, 715–717, 2010.
3. Gori, F., V. Ramirezsanchez, M. Santarsiero, and T. Shirai, "On genuine cross-spectral density matrices," *Opt. A: Pure Appl. Opt.*, Vol. 11, No. 8, 85706–85707, 2009.
4. Korotkova, O., S. Sahin, and E. Shchepakina, "Multi-Gaussian Schell-model beams," *J. Opt. Soc. Am. A*, Vol. 29, No. 10, 2159–2164, 2012.
5. Zhou, Y., Y. Yuan, J. Qu, and W. Huang, "Propagation properties of Laguerre-Gaussian correlated Schell-model beam in non-Kolmogorov turbulence," *Opt. Express*, Vol. 24, No. 10, 10682–10693, 2016.
6. Mei, Z. and O. Korotkova, "Random sources generating ring-shaped beams," *Opt. Lett.*, Vol. 38, No. 2, 91–93, 2013.
7. Wu, G., W. Dai, H. Tang, and H. Guo, "Beam wander of random electromagnetic Gaussian-shell model vortex beams propagating through a Kolmogorov turbulence," *Opt. Communications*, Vol 336, 55–58, 2015.
8. Tofsted, D., "Outer-scale effects on beam-wander and angle-of-arrival variances," *Appl. Opt.*, Vol. 31, No. 27, 5865–5870, 1992.
9. Zunino, L., D. Gulich, G. Funes, and D. Perez, "Turbulence-induced persistence in laser beam wandering," *Opt. Lett.*, Vol. 40, No. 13, 3145–3148, 2015.
10. Chen, X. and X. Ji, "Directionality of partially coherent annular flat-topped beams propagating through atmospheric turbulence," *Opt. Communications*, Vol. 281, No. 18, 4765–4770, 2008.
11. Gbur, G. and E. Wolf, "Spreading of partially coherent beams in random media," *J. Opt. Soc. Am. A*, Vol. 19, No. 8, 1592, 2002.
12. Yao, M., I. Toselli, and O. Korotkova, "Propagation of electromagnetic stochastic beams in anisotropic turbulence," *Opt. Express*, Vol. 22, No. 26, 31608–31619, 2014.
13. Wang, M., X. Yuan, J. Li, X. Zhou, Q. Li, and Z. Zhou, "Propagation of radial partially coherent beams in anisotropic non-kolmogorov turbulence," *Acta Optica Sinica*, Vol. 38, No. 03, 0306003, 2018.
14. Cui, L., B. Xue, and F. Zhou, "Generalized anisotropic turbulence spectra and applications in the optical waves' propagation through anisotropic turbulence," *Opt. Express*, Vol. 23, No. 23, 30088, 2015.
15. Cheng, M., L. Guo, J. Li, X. Yan, K. Dong, and Y. You, "Average intensity and spreading of a radially polarized multi-Gaussian Schell-model beam in anisotropic turbulence," *Quant. Spectrosc. Radiat. Transf.*, Vol. 218, 12–20, 2018.
16. Wang, F., C. Liang, Y. Yuan, and Y. Cai, "Generalized multi-Gaussian correlated Schell-model beam: from theory to experiment," *Opt. Express*, Vol. 22, No. 19, 23456, 2014.
17. Yuan, Y., X. Liu, F. Wang, Y. Chen, Y. Cai, and J. Qu, "Scintillation index of a multi-Gaussian Schell-model beam in turbulent atmosphere," *Opt. Communications* Vol. 305, No. 3, 57–65, 2013.
18. Zhang, Y., L. Liu, C. Zhao, and Y. Cai, "Multi-Gaussian Schell-model vortex beam," *Phys. Let. A*, Vol. 378, No. 9, 750–754, 2014.
19. Wang, F. and O. Korotkova, "Random optical beam propagation in anisotropic turbulence along horizontal links," *Opt. Express*, Vol. 24, No. 21, 24422–24434, 2016.
20. Bateman, H., A. Erdélyi, H. Haeringen, and L. Kok, *Tables of Integral Transforms*, 653–667, McGraw-Hill, New York, 1954.
21. Andrews, L. and R. Phillips, *Laser Beam Propagation through Random Media*, 2nd edition, 201–205, SPIE Press, Bellingham, 2005.